AMERICAN SOCIETY FOR MICROBIOLOGY | Infection and Immunity®

FUNGAL AND PARASITIC INFECTIONS

Genetic Adjuvantation of a Cell-Based Therapeutic Vaccine for Amelioration of Chagasic Cardiomyopathy

Vanaja Konduri,[a] Matthew M. Halpert,[a] Dan Liang,[a] Jonathan M. Levitt,[a,b,c] Julio Vladimir Cruz-Chan,[d,e,f] Bin Zhan,[d,e] Maria Elena Bottazzi,[d,e,g] Peter J. Hotez,[d,e,g] Kathryn M. Jones,[d,e] William K. Decker[a,c,d,h]

Department of Pathology and Immunology,[a] Scott Department of Urology,[b] Dan L. Duncan Cancer Center,[c] National School of Tropical Medicine,[d] Department of Pediatrics,[e] Department of Molecular Virology and Microbiology,[g] and Center for Cell and Gene Therapy,[h] Baylor College of Medicine, Houston, Texas, USA; Laboratorio de Parasitología, Centro de Investigaciones Regionales Dr. Hideyo Noguchi, Universidad Autónoma de Yucatán, Mérida, México[f]

ABSTRACT Chagas disease, caused by infection with the protozoan parasite *Trypanosoma cruzi*, is a leading cause of heart disease ("chagasic cardiomyopathy") in Latin America, disproportionately affecting people in resource-poor areas. The efficacy of currently approved pharmaceutical treatments is limited mainly to acute infection, and there are no effective treatments for the chronic phase of the disease. Preclinical models of Chagas disease have demonstrated that antigen-specific $CD8^+$ gamma interferon (IFN-γ)-positive T-cell responses are essential for reducing parasite burdens, increasing survival, and decreasing cardiac pathology in both the acute and chronic phases of Chagas disease. In the present study, we developed a genetically adjuvanted, dendritic cell-based immunotherapeutic for acute Chagas disease in an attempt to delay or prevent the cardiac complications that eventually result from chronic *T. cruzi* infection. Dendritic cells transduced with the adjuvant, an adenoviral vector encoding a dominant negative isoform of Src homology region 2 domain-containing tyrosine phosphatase 1 (SHP-1) along with the *T. cruzi* Tc24 antigen and *trans*-sialidase antigen 1 (TSA1), induced significant numbers of antigen-specific $CD8^+$ IFN-γ-positive cells following injection into BALB/c mice. A vaccine platform transduced with the adenoviral vector and loaded in tandem with the recombinant protein reduced parasite burdens by 76% to >99% in comparison to a variety of different controls and significantly reduced cardiac pathology in a BALB/c mouse model of live Chagas disease. Although no statistical differences in overall survival rates among cohorts were observed, the data suggest that immunotherapeutic strategies for the treatment of acute Chagas disease are feasible and that this approach may warrant further study.

KEYWORDS Chagas disease, dendritic cell, SHP-1

Chagas disease, also known as American trypanosomiasis, is caused by infection with the protozoan parasite *Trypanosoma cruzi* (1). It is a leading cause of heart disease in Latin America, with up to 10 million infected people in the Western Hemisphere (2). The disease burden of Chagas, based on disability-adjusted life years (DALYs), is five times greater than that of malaria and approximately one-fifth that of HIV/AIDS in the Latin American/Caribbean region (3). Additionally, the annual economic toll for the treatment of infected patients exceeds $7 billion globally (4). Most of the deaths and disability attributed to Chagas disease result from chronic Chagas cardiomyopathy (CCC) (5) which develops in approximately 30% of infected individuals years to decades after the initial infection due to the cascading effects of parasite-induced pathological

Received 21 February 2017 **Returned for modification** 3 April 2017 **Accepted** 21 June 2017

Accepted manuscript posted online 3 July 2017

Citation Konduri V, Halpert MM, Liang D, Levitt JM, Cruz-Chan JV, Zhan B, Bottazzi ME, Hotez PJ, Jones KM, Decker WK. 2017. Genetic adjuvantation of a cell-based therapeutic vaccine for amelioration of chagasic cardiomyopathy. Infect Immun 85:e00127-17. https://doi.org/10.1128/IAI.00127-17.

Editor John H. Adams, University of South Florida

Address correspondence to Kathryn M. Jones, kathrynj@bcm.edu, or William K. Decker, decker@bcm.edu.

K.M.J. and W.K.D. contributed equally to the preparation of the manuscript.

changes, including inflammation, cardiomyocyte hypertrophy, and fibrosis (6–8). CCC patients develop conduction disturbances associated with arrhythmias and sudden death or an end stage characterized by gross enlargement with high right or left ventricular apical aneurysm. Histologically, diffuse and patchy chronic myocarditis with mononuclear cell infiltrates and fibrosis is evident (9, 10). Two drugs, benznidazole and nifurtimox, have been used for treatment since the 1970s and have limited efficacy and significant side effects. Both drugs have up to 100% efficacy in congenital infection when administered within the first years of life and 65 to 80% efficacy in children treated during the acute phase. However, less than 35% efficacy is achieved in adults treated during the chronic phase (11, 12). A recent meta-analysis concluded that these drugs are of questionable efficacy in preventing the onset of chagasic cardiomyopathy, and almost 20% of patients fail to complete the months-long drug regimen due to significant associated toxicities (13–15). New chemotherapeutics, such as posaconazole, show promise in preclinical testing but have been of limited efficacy in human studies (12, 16). In a recent trial, trypanocidal therapy with benznidazole in patients with established Chagas cardiomyopathy significantly reduced serum parasite detection but did not significantly reduce cardiac clinical deterioration through 5 years of follow-up (17). Thus, there remains an urgent need to develop new therapies, including vaccines, to achieve sustained parasitological cure and a decreased incidence of sudden cardiac death.

Preclinical studies have revealed the essential role of antigen-specific immune responses, primarily T-cell responses, in the control of *T. cruzi* parasite burden and cardiac disease. Several candidate antigens, including SA85-L1, Tc52, *trans*-sialidase antigen 1 (TSA1), and Tc24, have shown efficacy in reducing parasitemia and endpoint cardiac pathology when used therapeutically (18–21). These reductions in parasite burden, cardiac disease, and mortality are due to T_H1-type T-cell immunity and in part to the induction of antigen-specific $CD8^+$ T-cell responses (18, 22). To date, vaccines that combine Tc24 and TSA1 have provided the most dramatic reductions in parasite loads and cardiac inflammation in preclinical experimental systems. Mice vaccinated therapeutically during the acute phase with a combination Tc24-TSA1 DNA vaccine exhibited up to a 75% reduction in peak parasitemia, an approximately 60% reduction in cardiac parasite burden, and a significant reduction in endpoint cardiac pathology in comparison to unvaccinated mice (18, 20, 21). Similarly, mice vaccinated with a combination vaccine during the chronic phase demonstrated up to 80% survival at 180 days postinfection (dpi) and reduced endpoint cardiac pathology (20, 21, 23). Additionally, in a dog model of Chagas disease, the same therapeutic DNA vaccine construct reduced the number of dogs that developed cardiac arrhythmias at 50 days postinfection by 40% (24). Similar studies have shown protective efficacy using the recombinant protein counterparts of these DNA vaccines (2, 25–27).

Dendritic cells (DCs) are the most important of the professional antigen-presenting cells (APCs) that initiate and direct adaptive immune responses. Upon the detection of danger signals, DCs migrate to local lymph nodes where they induce a variety of immunogenic responses (28–32). Signals induced by the ligation of pattern recognition receptors, major histocompatibility complex (MHC) molecules, costimulatory molecules, and inflammatory cytokine receptors activate DCs, enabling them to drive immunogenic T-cell responses (33). Src homology region 2 (SH2) domain-containing tyrosine phosphatase 1 (SHP-1) is expressed in a wide variety of immune cells, where it plays a largely inhibitory role in cell signaling initiated through a range of stimuli (34). SHP-1 inhibition in DCs leads to increased proinflammatory cytokine production and the activation of Akt, enhancing DC survival. Importantly, mice vaccinated with SHP-1-inhibited DCs mount effective immune responses against both melanoma and prostate tumors, demonstrating that SHP-1 is an intrinsic negative regulator of DC activation signaling. Previous work demonstrated that a dominant negative kinase-inactivated SHP-1 adjuvant (dnSHP) delivered to DCs by means of an adenoviral vector could substantially enhance downstream T-cell responses in the context of vaccination (35).

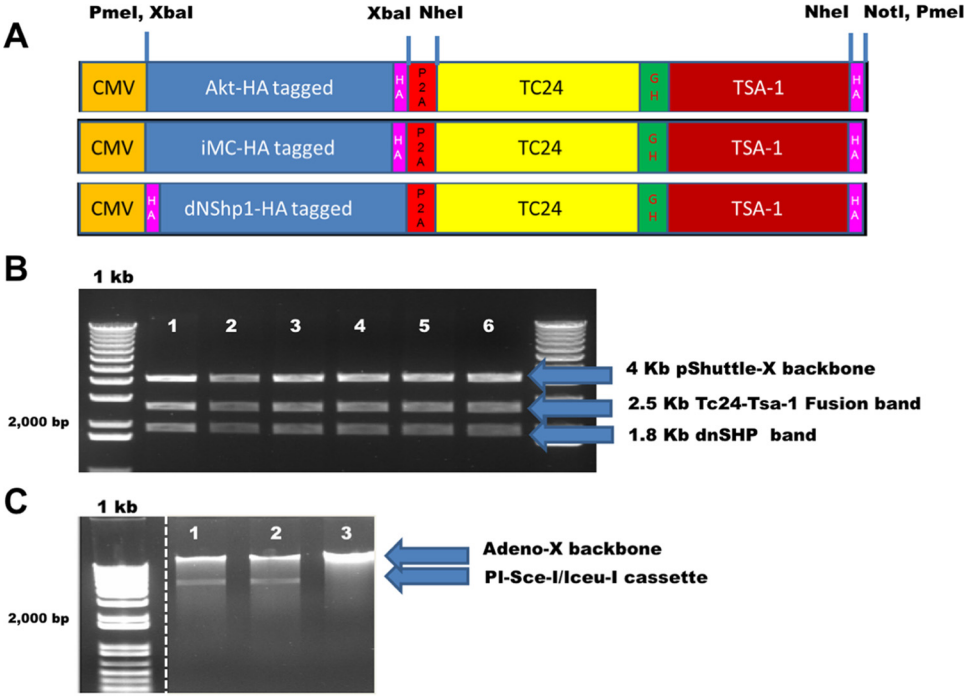

FIG 1 Bicistronic adenoviral constructs encoding functional adjuvants and parasite-specific antigens. Replication-deficient human recombinant adenovirus type 5 vectors were constructed with the genetic adjuvants caAKT (constitutively activated Akt), iMC (inducible MyD88/CD40), or dnSHP (dominant negative SHP-1) upstream of the *T. cruzi* antigens Tc24 and TSA1. (A) HA-tagged genetic adjuvants (Akt, iMC, and dnSHP) were cloned into the XbaI site of the pShuttle plasmid driven by the cytomegalovirus (CMV) promoter. The *T. cruzi* antigens Tc24 and TSA1 were cloned as a fusion fragment downstream of the adjuvants between the NheI and NotI sites. A single glycine hexamer linker separated the antigens, while a P2A sequence inserted between the antigens and adjuvant permitted the cleavage of the two. The expression cassette was cloned into the PmeI site of the pShuttle plasmid. (B) Restriction digestion of ampicillin-resistant positive shuttle plasmid clones with PmeI and XbaI generated the shuttle backbone fragment (4 kb), a fragment corresponding to the adjuvant (1.8 kb), and a fusion fragment corresponding to the antigens (2.5 kb). The clones were later confirmed by direct sequencing. (C) PsceI and IceuI digestion of the shuttle plasmid released the construct, which was then ligated into the adenoviral backbone according to the manufacturer's instructions. Ampicillin-resistant clones were selected, and further confirmation of the positive clones was performed by means of PsceI and IceuI restriction digestion followed by direct sequencing. The standard 1-kb ladder indicates the DNA fragment size with a doublet at 2.0 and 1.65 kb. The dotted line between the 1-kb ladder and shuttle plasmid digestions indicates the absence of irrelevant, unrelated digestion lanes spliced out of the image.

A therapeutic vaccine is a promising alternative intervention to delay or halt the progression of chagasic cardiomyopathy due to the high toxicities and poor efficacies of current pharmaceutical interventions (13, 14). Several vaccine platforms, including plasmid DNA, viral vectors, and recombinant proteins, have been pursued in preclinical studies and have demonstrated the ability to induce antigen-specific $CD8^+$ responses against viral and protozoal pathogens (36–38). In the present proof-of-principle study, we demonstrated that a candidate cell-based vaccine combining the *T. cruzi*-specific antigens Tc24 and TSA1 with the genetic adjuvant dnSHP exhibits therapeutic efficacy against *T. cruzi* infection and the ability to ameliorate cardiac pathology in a rodent model of Chagas disease.

RESULTS

Bicistronic adenoviral constructs encoding functional adjuvants and parasite-specific antigens. Shuttle plasmids were constructed with the *T. cruzi* antigens Tc24 and TSA1 downstream of the genetic adjuvants caAKT (constitutively activated Akt) (39), iMC (inducible MyD88/CD40) (40), and dnSHP (35) (Fig. 1A). Ampicillin-resistant positive clones were sequenced, followed by restriction digestions with XbaI and PmeI to confirm successful cloning (Fig. 1B). The constructs were excised from the shuttle plasmid backbone and ligated into the adenoviral backbone according to the manu-

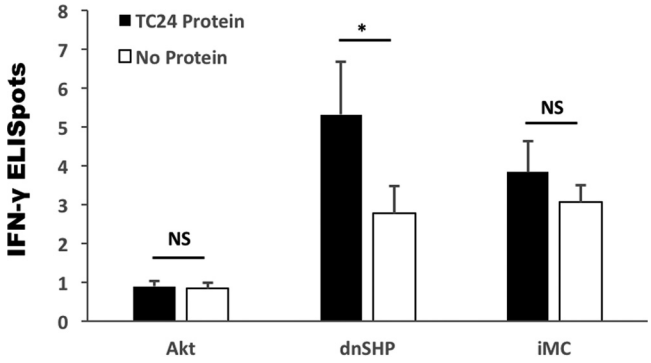

FIG 2 Genetic adjuvantation with dnSHP induces significantly enhanced antigen-specific IFN-γ responses. Mice were vaccinated with each of the adenoviral constructs (caAKT-TC24/TSA1, iMC-TC24/TSA1, and dnSHP-TC24/TSA1), and antigen-specific responses were measured by the IFN-γ secretion of splenocytes stimulated with and without 10 μg/ml Tc24 protein by an ELISpot assay. Compared to caAKT and iMC, genetic adjuvantation with dnSHP induced a significant enhancement of the production of Tc24-specific IFN-γ responses. NS, not significant; *, $P \leq 0.05$.

facturer's instructions. Ampicillin-resistant clones were selected, and confirmation of positive clone selection was performed by means of Psce-I and Iceu-I restriction digestion followed by direct sequencing (Fig. 1C). We next tested the efficacy of each adenoviral construct in generating antigen-specific immune responses. Mice were vaccinated with each of the adenoviral constructs (caAKT [constitutively activated Akt]-TC24/TSA1, iMC-Tc24/TSA1, and dnSHP-Tc24/TSA1), and antigen-specific responses were measured by gamma interferon (IFN-γ) secretion by restimulated splenocytes. Compared to caAKT and iMC, genetic adjuvantation with dnSHP gave a significantly better enhancement of the production of Tc24-specific IFN-γ responses (Fig. 2). Low-titer adenovirus was produced for the construct with dnSHP as the genetic adjuvant. Western blot analysis of HEK293T cells and DCs transduced with viral particles (vp) and probed with antihemagglutinin (anti-HA), anti-SHP-1, anti-Tc24, and anti-TSA1 proteins confirmed the expression of the genetic adjuvant and/or antigenic fusion protein (Fig. 3A to D). DCs were transduced with different titrations of the viral particles, and cell lysates were probed with anti-SHP-1 antibody to determine the optimum titer at which the antigen, adjuvant, and fusion proteins could be detected. We observed that good expression could be obtained by transducing DCs with doses as low as 100 vp (10^2 vp) per cell (Fig. 3E) as described previously (39).

DC vaccines transduced with the dnSHP adenoviral construct and loaded with the Tc24 recombinant protein reduce *T. cruzi* parasite burdens and significantly improve cardiac pathology. To test the therapeutic efficacy of the dnSHP-based DC vaccine, mice were challenged intraperitoneally (i.p.) with 500 blood-form *T. cruzi* trypomastigotes and treated therapeutically 7 days later by using a variety of different DC-based platforms. These platforms included unloaded DCs, DCs transduced with the dnSHP vector alone, DCs loaded with only the Tc24 recombinant protein, DCs transduced with the dnSHP vector and simultaneously loaded with the Tc24 recombinant protein to provide antigen-specific T-cell help (41–43), as well as untreated controls (Fig. 4A). Following infection and treatment, mice were monitored for 50 days and then sacrificed for analysis. Most mice lived until day 50; however, a few died prior to day 50 and were not available for all analyses. Although a Kaplan-Meier survival plot is provided in Fig. S1A in the supplemental material, there were no statistically significant differences in overall survival rates observed between groups. Analysis of serum antibody titers (Fig. 4B) demonstrated that mice treated with vector- and protein-loaded DCs exhibited significantly elevated Tc24-specific IgG1 antibody titers ($P < 0.004$). Mice treated by any other means exhibited IgG1 titers indistinguishable from those stimulated by infection alone. There were no statistically significant differences observed among Tc24-specific IgG2a or IgG2b antibody isotype titers, nor were there significant differences observed in total Tc24-specific serum IgG levels (not shown).

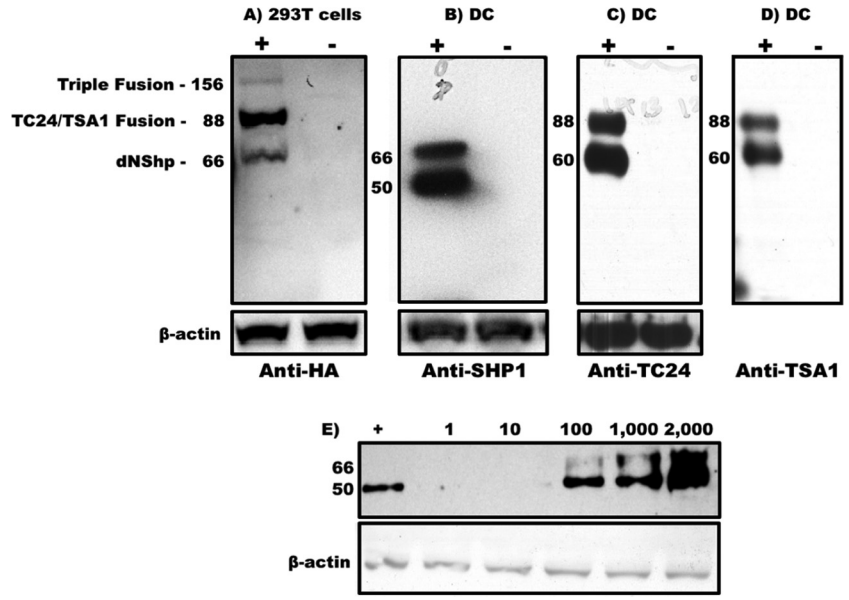

FIG 3 Expression of the genetic adjuvant and parasite-specific antigens in DCs transduced with the adenoviral vector. Low-titer adenovirus was made with dnSHP as the genetic adjuvant. (A to D) HEK293T cells and dendritic cells were transduced with adenovirus expressing dnSHP (genetic adjuvant) and Tc24 and TSA-1 (antigens). Western blots of cell lysates were probed with anti-HA, anti-SHP, anti-Tc24, and anti-TSA1 antibodies to confirm the expression of the adjuvant, antigen, and fusion protein products. (E) Dendritic cells were transduced with different titrations of the viral particles, and cell lysates were probed with anti-SHP-1 antibody. Doses as low as 100 vp (10^2 vp) per cell gave good expression of the adjuvant, as confirmed by Western blotting. Protein molecular masses (in kilodaltons) are indicated on the left-hand side of each blot.

Furthermore, there were no statistically significant differences in IFN-γ-secreting T cells in peripheral circulation, as evidenced by an IFN-γ enzyme-linked immunosorbent spot (ELISpot) assay (not shown).

Despite the only modest immunological differences observed between groups on study day 50, there were significant differences observed with regard to objective cardiac pathology. Quantitative PCR (qPCR) analysis of cardiac samples using *T. cruzi*-specific primers indicated a clear trend toward low levels of or no detectable parasite DNA among mice that received vector- and protein-loaded DCs (76% less parasite DNA than in protein-only DCs, 80% less than in vector-only DCs, and >99% less than in either unloaded DCs or unvaccinated controls) (Fig. 4C), despite the lack of clear differences in blood-form parasite burdens between groups (Fig. S1B; the area under the parasitemia curve is shown for each animal in Fig. S1C). Hematoxylin-and-eosin (H&E)-stained cardiac tissues were scored for lymphocytic infiltration in a randomized and blind fashion. A score of 0 indicated minimum or no infiltration, and a score of 5 indicated maximum infiltration. The pathological scoring demonstrated that mice that received vector- and protein-loaded DCs exhibited substantially lower pathological index scores (Fig. 4D), some on par with those of uninfected mice ($P < 0.0006$). Furthermore, cardiac size (enlargement) as assessed by multiple measurements of the gross cross-sectional distance was nearly 20% smaller (5.04 mm versus 6.16 mm; $P < 0.0001$) among mice that received vector- and protein-loaded DCs and similar to that of uninfected mice (Fig. 4E). Representative images indicating the cardiac histopathology of each group at a magnification of ×100 are shown in Fig. 5A to E, and the presence of amastigote nests is shown in images at a ×400 magnification in Fig. 5F to J. Significant numbers of amastigote nests were observed in at least one animal of each of the five groups, with the exception of the vector- and protein-loaded DC group, in which no amastigote nests were observed in any sample from any animal. The presence of inflammatory fibrosis was also characterized by Masson's trichrome staining with blind image capture and ImageJ quantitation. As indicated in the representative images

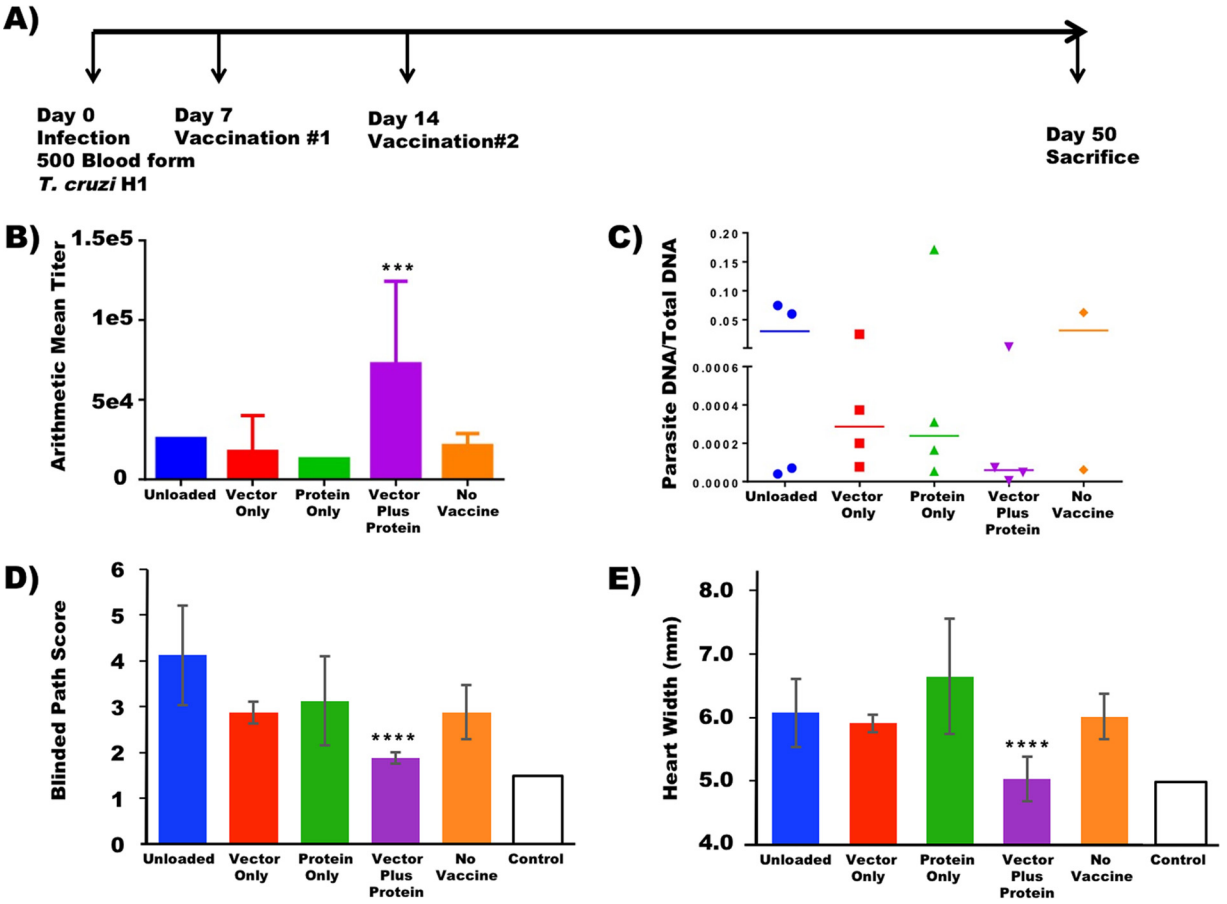

FIG 4 DC vaccines transduced with the dnSHP adenoviral construct and loaded with the recombinant Tc24 protein reduce the *T. cruzi* parasite burden. (A) To test the therapeutic efficacy of the vaccine, naive BALB/c mice were infected intraperitoneally with 500 blood-form trypomastigotes. At 7 dpi, the mice were therapeutically immunized intraperitoneally with 250,000 DCs transduced with the dnSHP vector alone, DCs loaded with the recombinant Tc24 protein only, and DCs transduced with the dnSHP vector and simultaneously loaded with the recombinant Tc24 protein. Unloaded DCs served as controls. Boost vaccination was given at 14 dpi. At 50 dpi, all remaining mice were sacrificed and analyzed. (B) Serum antibody titers analyzed for the mice at the end of the study demonstrate that mice treated with vector-plus-protein-loaded DCs exhibited significantly elevated Tc24-specific IgG1 antibody titers ($P < 0.004$). (C) Endpoint cardiac parasite DNA was quantified by qPCR analysis using *T. cruzi*-specific primers. A trend toward low/no detectable parasite DNA ($P = 0.08$) was observed among mice that received vector-plus-protein-loaded DCs compared to the other groups. (D and E) H&E staining was performed on cardiac tissue at the end of the study, and pathological scores on a scale of 0 to 5 were given for lymphocytic infiltration, with 5 being maximum infiltration. Randomized and blind pathological scoring demonstrated that mice which received vector-plus-protein-loaded DCs exhibited substantially lower pathological index scores, some on par with those of uninfected mice ($P < 0.0006$). The endpoint cardiac size (enlargement) as assessed by cross-sectional distance was nearly 20% smaller (5.04 mm versus 6.16 mm; $P < 0.0001$) among mice that received vector-plus-protein-loaded DCs and similar to that of uninfected mice. For all panels, error bars indicate SEM.

(Fig. 5K to O), extensive inflammatory damage was observed in all groups except for the vector-plus-protein group and, to a lesser extent, the unvaccinated group. Nonetheless, among infected animals, the level of trichrome staining was significantly lower only in the vector-plus-protein group ($P < 0.01$ by one-way analysis of variance [ANOVA]) (Fig. 6).

DISCUSSION

The objective of the present proof-of-principle study was to determine the therapeutic efficacy of DC-based vaccines to prevent the progression of acute Chagas disease to chagasic cardiomyopathy. Vaccines using replication-deficient human recombinant type 5 adenoviruses have been viewed as an attractive strategy to deliver antigens for the generation of specific immune responses. In the present study, antigen-specific cellular immune responses against Tc24 were observed following vaccination with an adenoviral vector-transduced dendritic cell-based vaccine, further substantiating the use of adenoviral vectors for DNA delivery. This study made use of

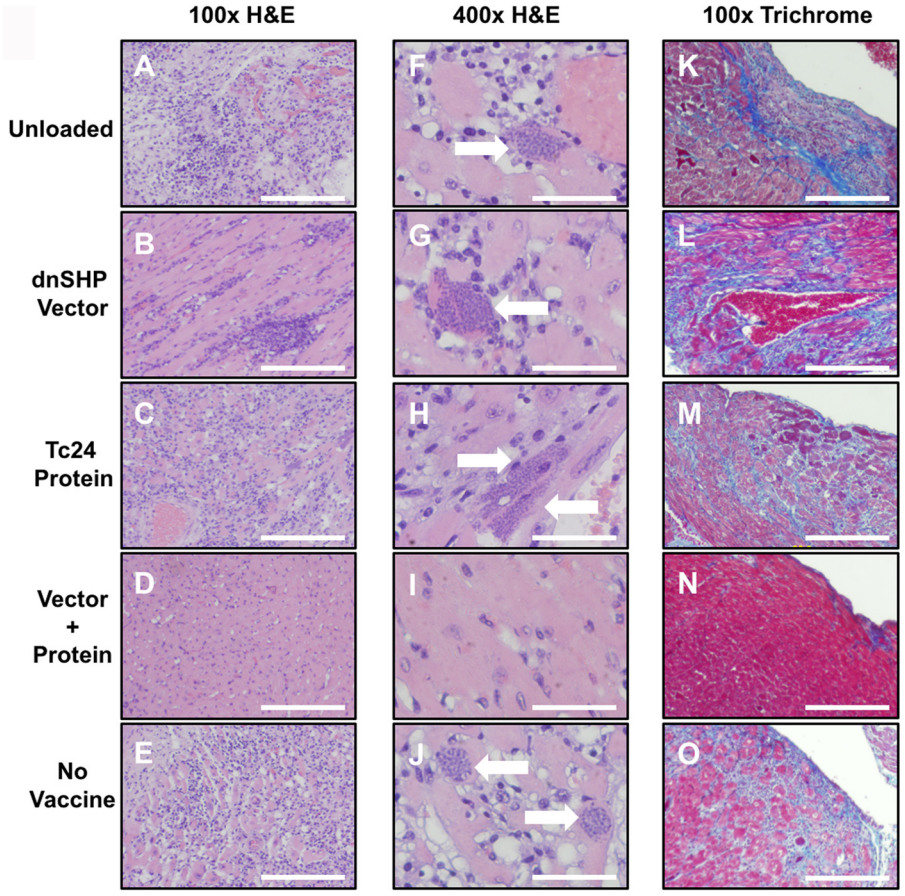

FIG 5 DC vaccines transduced with the dnSHP adenoviral construct and loaded with the recombinant Tc24 protein improve cardiac pathology. (A to E) Representative endpoint cardiac H&E histopathology reveals amastigote nest formation in mice from all groups except the ones treated with DCs loaded with the vector and protein. Images are shown at a ×100 magnification. Bar = 20 μm. (F to J) Representative H&E-stained images of the amastigote nests in cardiac tissues of each group of mice. Images are shown at a ×400 magnification. Bar = 5 μm. (K to O) Representative Masson's trichrome-stained images showing the extent of cardiac inflammatory fibrosis among mice of each treated group. Images are shown at a ×100 magnification. Bar = 20 μm.

the *in vitro* transduction of dendritic cells, thereby bypassing legitimate concerns about the ability of preexisting adenovirus type 5 (Ad5)-neutralizing antibody titers to hinder or abolish *in vivo* transduction in previously exposed individuals. Genetic adjuvantation is an attractive strategy by which to augment the generation of immune responses (44).

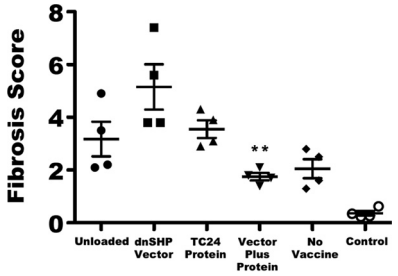

FIG 6 Quantitation of Masson's trichrome staining. To quantify cardiac fibrosis, 5-μm sections of heart tissue were stained with Masson's trichrome stain. Images of three to five representative sections from each mouse were captured at a ×100 magnification by using a Fisher Micromaster microscope and Micron software. Images were evaluated by a reviewer who was blind to the treatment groups and analyzed by using ImageJ FIJI software to quantify the area of fibrosis and the total tissue area. The level of fibrosis in the vector-plus-protein group was significantly lower than those in all other infected groups as determined by one-way ANOVA (**, $P < 0.01$). Data for uninfected age-matched control mice are shown at the far right for comparison. Error bars indicate SEM.

SHP-1 is expressed in a wide variety of immune cells, where it plays a largely inhibitory role in cell signaling (34). Previous work showed that DCs transduced with a dominant negative kinase-inactivated SHP-1 adjuvant (dnSHP) can substantially enhance antitumor T-cell responses in the context of cancer vaccination (35), suggesting that such a strategy might be beneficial in enhancing T-cell-mediated immunity against other diseases. However, natural mutation of SHP-1 is also known to result in several characteristic autoimmune phenotypes that vary in severity from enhanced dermatitis to early postnatal death (35, 45, 46). Despite this theoretical potential for the development of autoimmune inflammation, no such inflammation was observed in previous studies (35) or in the present studies, regardless of whether the genetic adjuvant was delivered to mice by *in vivo* plasmid transfection, *in vivo* adenoviral transduction, or administration of pretransduced dendritic cells.

The administration of DNA vaccines encoding a *trans*-sialidase antigen (TSA1) or the secreted antigen Tc24 (47) following *T. cruzi* infection was able to reduce parasitemia and cardiac inflammatory reactions while increasing the survival of treated mice (48). Therapeutic DNA vaccination with plasmids encoding Tc24 and TSA1 has demonstrated efficacy across different strains of mice, with no antigenic interference and/or genetic restriction of vaccine efficacy (18). As in mice, the therapeutic administration of two doses of DNA vaccines encoding TSA1 and Tc24 during the acute phase was also tested in dogs, and electrocardiogram (EKG) recordings indicated a decrease in the severity of disease-associated cardiac arrhythmia (49). In the present study, we demonstrate that the expression of the Tc24 and TSA1 antigens through dendritic cell-based vaccination generated effective antigen-specific immune responses that not only aided in parasite clearance but also mitigated cardiac manifestations of the parasite. In this model system, vaccination with MHC class I and II presentation of Tc24 and TSA1 significantly decreased the total fibrotic cardiac tissue area and overall heart width. Detailed studies of the chagasic infection process *in vitro* have shown that invasion of *T. cruzi* into cardiac cells induces hypertrophy and increased production of collagen IV and fibronectin (50). Furthermore, *T. cruzi* invasion activates transforming growth factor β (TGF-β), inducing intracellular signaling cascades that can drive the expression of profibrotic genes (51–55). Thus, we propose that vaccine efficacy can be attributed in part to the induction of an immune response that enhances parasite killing, decreasing total cardiomyocyte invasion by *T. cruzi* with a concomitant reduction of TGF-β-activated profibrotic gene expression.

Other animal models are available for the study chagasic cardiomyopathy, including canine and nonhuman primate models (49, 56–58). These models possess much if not all of the cardiac pathology seen in classic human chagasic cardiomyopathy. However, rodents are also a widespread natural reservoir for the parasite, and laboratory mice have been used extensively to study vaccine efficacy as well as the effects of *T. cruzi* on cardiac pathology induced by both acute and chronic Chagas disease (20, 22). Inbred rodent models also represent the most accurate, cost-effective, and reproducible systems with which to effectively model translational research with statistically reliable results.

The generation of differential IgG subclasses has been indicated in antibody responses (59, 60) as well as CD8 responses (61, 62) after *T. cruzi* infection. In the present study, analysis of the IgG subclasses from mice immunized with the adenoviral dendritic cell vaccine indicated that IgG1 was the dominant response in immunized BALB/c mice. In a previous study by Farrow et al. (63), a strong IgG2b response induced by the Ad5-gp83 vaccine facilitated antibody-dependent cellular cytotoxicity (ADCC) and complement-dependent cytotoxicity in addition to eliciting neutralizing antibodies. Coordinated cellular (T_H1) and humoral (T_H2) responses are important for the effective clearance of intracellular pathogens by the adaptive immune system. In conjunction with an adjuvant, protective T_H2 immunity can be achieved by the administration of antigens. In the case of intracellular infection, protective cell-based responses can be generated only by the administration of an attenuated live pathogen that induces subclinical infection. In the present study, we observed that the loading of DCs with

adenovirus and recombinant protein together resulted in a significant amelioration of cardiac pathology in comparison to that of mice that received DCs loaded by any other means. While the reasons for this observation are not elucidated here, they may be related to the previously observed and reported phenomenon of homologous T-cell help (41–43).

Interestingly, some of the vaccinated groups in this acute model developed significant cardiac fibrosis. Evident fibrosis takes time to occur, and with only 7 weeks between inoculation and sacrifice, significant cardiac fibrosis was an unexpected finding. Cardiac fibrosis is not caused directly by the pathogen itself but by T_H2-biased (64–66) and T_H17-biased (67–70) immune responses mounted against *T. cruzi* over time. Vaccination of mice with individually loaded vector and protein vaccines appeared to accelerate the development of the T_H2- and T_H17-biased responses that are well-known mediators of fibrosis. In contrast, vaccination of mice with vector-plus-protein-loaded DCs, a methodology that we previously showed (41–43) promotes antifibrotic T_H1-biased (71–73) responses, did not generate significant fibrotic damage. Given that there was no vaccine-mediated acceleration of pathogen-specific immune responses among unvaccinated mice, the level of fibrotic damage in this group was also relatively low. Presumably, unvaccinated mice would have eventually developed levels of cardiac fibrosis similar to those of the vector-only- and protein-only-loaded groups if they were sacrificed at a significantly later time point. This result provides a cautionary tale for others attempting the amelioration of Chagas disease by immunotherapeutic means. T_H1-polarized adaptive responses may be important, not solely for control of the pathogen but also for the minimization of immune-mediated damage to vital cardiac tissue.

The mouse model of acute *T. cruzi* H1 infection used for these studies is well established and has been shown by several investigators to induce detectable parasitemia, cardiac parasites, and cardiac inflammation (18, 20, 25, 26). While we found that the dendritic cell vaccine construct did not result in appreciable reductions in blood parasite burdens, we observed a significant reduction in cardiac inflammation, which would translate to improved cardiac health. The parasite burden following immunosuppression would be an important parameter to evaluate if there was evidence that the treatment reduced blood parasite burdens to undetectable levels at key time points, for example, at the expected time of peak parasitemia (74, 75). However, in our model, the blood parasite burden was not reduced to undetectable levels, and thus, there was not strong evidence that sterilizing immunity had been achieved. Furthermore, the vaccine construct used in this model is consistent with DNA- and protein-based vaccines using the Tc24 and TSA1 antigens that achieve immune control of the parasites and significantly reduce parasite burdens and cardiac pathology but without achieving sterilizing immunity (20, 21, 25, 26). As 60 to 70% of chronically infected individuals naturally remain in the indeterminate stage without ever developing CCC, many hypothesize that immune control of the parasite through vaccination or other immune modulation, without the complete elimination of the parasite, remains a viable option for reducing the disease burden and improving cardiac health (2, 27). Despite the fact that sterilizing immunity was likely not achieved with the dendritic cell vaccine constructs described here, the results nonetheless demonstrate that the generation of antigen-specific immune responses against *T. cruzi* infection through genetic adjuvantation can successfully mitigate cardiac pathology associated with chagasic cardiomyopathy and that follow-up studies are warranted.

MATERIALS AND METHODS

Construction of an adenoviral vaccine vector. The construction of the replication-deficient human recombinant adenovirus type 5 vector carrying the genetic adjuvants caAKT (constitutively activated Akt) (39), iMC (inducible MyD88/CD40) (40), or dnSHP (dominant negative SHP-1) (34) upstream of the *T. cruzi* antigens Tc24 (GenBank accession number U70035) and TSA1 (GenBank accession number M58466) was performed as described previously (76). Briefly, HA-tagged genetic adjuvants (Akt, iMC, and dnSHP), generated as described previously (35, 39, 40), were amplified by PCR using XbaI-flanked primers and cloned into the XbaI site of the pShuttle plasmid. The *T. cruzi* antigens Tc24 and TSA1 were cloned as a PCR-generated fusion fragment downstream of the adjuvants between the NheI and NotI sites. A single

primer-encoded glycine hexamer linker separated the antigens, while a primer-encoded P2A sequence inserted between the antigens and adjuvant permitted the cleavage of the two (47). The expression cassette was digested and cloned into the PmeI site of the pShuttle plasmid. The cassette was excised by using the unique restriction sites PsceI and IceuI and ligated into the Adeno-X backbone. By using the BD Adeno-X system, low-titer adenovirus was made by transfecting HEK293 cells with the pAdenoX construct expressing the *T. cruzi*-specific antigens according to the manufacturer's instructions (BD Biosciences, San Jose, CA).

Western blotting and analysis. All gel electrophoreses were performed under denaturing, reducing conditions on a 12% polyacrylamide gel, with subsequent transfer to a 0.45-μm nitrocellulose membrane for antibody probing. All blocking and antibody staining steps were carried out with 5% milk, and primary antibodies were applied overnight at 4°C. The Western blot chemiluminescent signal was detected by using a ChemiDoc XRS digital imaging system supported by Image Lab software version 2.0.1 (Bio-Rad Laboratories, Hercules, CA). All Western blots were quantitated by densitometry of Ponceau S (Sigma-Aldrich, St. Louis, MO)-stained membranes. Contamination of supernatants with residual cell lysate or debris from cell death was controlled for by immunoblotting with anti-β-actin (Santa Cruz Biotechnology, Dallas, TX) and additional densitometry. Densitometry was performed by using ImageJ software (NIH, Bethesda, MD). All Western blots are representative of results from at least three independent experiments.

Vaccine production. DCs were generated from BALB/c mice. Bone marrow leukocytes were flushed from mouse tibia and femur and cultured in AIM-V containing 10% fetal bovine serum (FBS) and 1% antibiotics and supplemented with 50 ng/ml murine granulocyte-macrophage colony-stimulating factor (mGM-CSF) and 10 ng/ml murine interleukin-4 (mIL-4) for 3 days. Cells were cultured in a humidified chamber at 37°C with 5% atmospheric CO_2. The culture medium was removed and replenished with an equal volume of fresh medium supplemented with cytokines on day 3. On day 5, the cells were replenished with fresh AIM-V containing 10% mouse serum and 1% penicillin-streptomycin-amphotericin (anti-anti) and supplemented with mGM-CSF and mIL-4 (R&D Systems, Minneapolis, MN). Immature DCs were harvested on day 6, counted, and incubated with adenovirus (expressing the Tc24 and TSA1 antigens and dnSHP as a genetic adjuvant) and recombinant Tc24 protein (25) (10 μg/ml) in AIM-V supplemented with 5% mouse serum for 3 h. The virus was added to the cells at a concentration of 1,000 viral particles per DC. Cells were plated in a six-well plate at 10^6 cells/well in AIM-V supplemented with 5% mouse serum. After 3 h of incubation, DCs were allowed to mature for 24 h in AIM-V supplemented with 10% mouse serum, 50 ng/ml GM-CSF, 10 ng/ml IL-4, 10 ng/ml IL-1β (R&D Systems), 10 ng/ml tumor necrosis factor alpha (TNF-α) (R&D Systems), 15 ng/ml IL-6 (R&D Systems), and 1 μg/ml prostaglandin E_2 (PGE_2) (Sigma-Aldrich). The final DC product was extensively characterized as described previously (41, 77).

Mice, parasites, and infection model. Six- to eight-week-old female BALB/c mice were obtained from Harlan Laboratories (Houston, TX). All mice were maintained in accordance with the specific IACUC requirements of the Baylor College of Medicine (animal welfare assurance number A-3823-01) and in specific accordance with IACUC-approved protocol AN-5973. *T. cruzi* H1 strain parasites, previously isolated from a human case in Yucatan, Mexico, were maintained by serial passage in mice. Naive mice were infected intraperitoneally with 500 blood-form trypomastigotes as previously described and validated (20). At 7 dpi, the mice were immunized intraperitoneally with 250,000 DCs loaded with adenoviral particles and the Tc24 protein. Blood was collected twice weekly for the quantification of parasitemia. At 50 dpi, all remaining mice were sacrificed and analyzed.

Vaccination, blood draws, and parasitemia. Seven days after parasite challenge, cohorts of 4 to 5 mice each received primary vaccination with 250,000 DCs per mouse intraperitoneally. Boost vaccination was given 7 days later (41, 77). Blood was collected from the tail vein twice per week, and parasitemia was quantitated by visual microscopy and qPCR using primers specific for *T. cruzi* nuclear DNA (78). Serum was collected at every blood draw for downstream analysis. Heart tissue was collected on the day of sacrifice for histopathology and qPCR analyses. The experiment characterized is one of three different iterations.

IFN-γ ELISpot assays. Tc24-specific IFN-γ-producing splenocytes were quantified by an ELISpot assay after overnight bulk restimulation with Tc24-loaded DCs using the IFN-γ ELISpot Plus kit (Mabtech, Inc., Cincinnati, OH) according to the manufacturer's instructions. Briefly, filter plates were coated overnight with 15 μg/ml coating antibody. Plates were blocked with Dulbecco's modified Eagle's medium (DMEM) supplemented with 10% FBS at room temperature. Cells and stimuli were added to the plate in a final volume of 0.2 ml. Cells were used at final concentrations of 2.5×10^5 cells per well with 5 μg/ml concanavalin A, 10 μg/ml Tc24 protein, or medium only (DMEM supplemented with 5% FBS and 1$\times$ penicillin-streptomycin). The plate was incubated for approximately 18 h at 37°C in 5% CO_2. The amount of bound IFN-γ was quantified by using 1 μg/ml biotinylated detection antibody, a 1:1,000 dilution of streptavidin-horseradish peroxidase (HRP), and the TMB substrate. After drying for a minimum of 18 h, spots were counted manually by using a dissecting microscope.

Serum antibody titers. Serum antibodies to Tc24 were measured by an enzyme-linked immunosorbent assay (ELISA). Plates were coated with 1.25 μg/ml Tc24 protein in coating solution. Plates were blocked, and serially diluted serum samples were added. Bound antibody was detected with a 1:4,000 dilution of HRP-conjugated goat anti-mouse total IgG, IgG1, or IgG2a secondary antibody. The reaction was developed with the TMB substrate (Thermo Fisher Scientific, Waltham, MA). Titers were recorded as the last positive dilution above a cutoff optical density (OD) as determined by the OD at 450 nm (OD_{450}) plus 3 standard deviations (SD) for serum from naive mice.

Evaluation of parasite burdens. Total DNA was isolated from blood or tissue by using a DNeasy blood and tissue kit (Qiagen, Valencia, CA). *T. cruzi* levels from 10 ng blood DNA or 50 ng heart tissue DNA were measured by quantitative real-time PCR using TaqMan Fast Advanced master mix (Life Technologies, Carlsbad, CA) and oligonucleotides specific for the satellite region of *T. cruzi* nuclear DNA (primers 5′-ASTCGGCTGATCGTTTTCGA-3′ and 5′-AATTCCTCCAAGCAGCGGATA-3′ and probe 5′-FAM [6-carboxyfluorescein]-CACACACTGGACACCAA-MGB-3′ [catalog numbers 4304972 and 4316032; Life Technologies]) (41, 78). Data were normalized to values for glyceraldehyde-3-phosphate dehydrogenase (GAPDH) (primers 5′-CAATGTGTCCGTCGTGGATCT-3′ and 5′-GTCCTCAGTGTAGCCCAAGATG-3′ and probe 5′-FAM-CGTGCCGCCTGGAGAAACCTGCC-MGB-3′; Life Technologies) (79), and parasite equivalents were calculated based on a standard curve as described previously (80, 81).

Evaluation of cardiac pathology. Heart tissue was removed from euthanized animals and fixed in 10% formaldehyde for histopathological analysis. Samples were embedded in paraffin, cut into 5-μm sections, and stained with hematoxylin and eosin. For each mouse, a representative section was identified, and amastigote nests were quantified over 20 fields of view at a $\times$400 magnification in a blind fashion. Lymphocytic infiltration in the representative sections was scored on a scale of 0 to 5, with 0 being minimum or no infiltration and 5 being maximum infiltration (22). Heart enlargement was determined by measurement of multiple cross-sectional slices ($>$3 for each animal) taken from the center of each paraffin block.

Quantification of cardiac fibrosis. Heart samples were fixed in 10% neutral buffered formalin and embedded in paraffin. To measure cardiac fibrosis, 5-μm sections were adhered to glass slides and stained with Masson's trichrome stain. Images of three to five representative sections from each mouse were captured at a $\times$100 magnification by using a Fisher Micromaster microscope and Micron software. Images were evaluated by a reviewer blind to the treatment groups and analyzed by using ImageJ FIJI software to quantify the area of fibrosis and the total tissue area.

Statistical analysis. Statistical significance was determined by Student's two-tailed *t* test or one-way ANOVA using Prism software (GraphPad Software, La Jolla, CA). Survival was analyzed by means of Kaplan-Meier analysis. Bonferroni correction was applied when necessary to control for type I errors during multiple comparisons. Data are presented as the means $\pm$ standard errors of the means (SEM) unless stated otherwise. Statistical significance was defined as a P value of $\leq$0.05.

SUPPLEMENTAL MATERIAL

Supplemental material for this article may be found at https://doi.org/10.1128/IAI.00127-17.

SUPPLEMENTAL FILE 1, PDF file, 0.1 MB.

ACKNOWLEDGMENT

This work was supported by funding from the Carlos Slim Foundation.

REFERENCES

1. Hotez PJ, Dumonteil E, Woc-Colburn L, Serpa JA, Bezek S, Edwards MS, Hallmark CJ, Musselwhite LW, Flink BJ, Bottazzi ME. 2012. Chagas disease: "the new HIV/AIDS of the Americas." PLoS Negl Trop Dis 6:e1498. https://doi.org/10.1371/journal.pntd.0001498.
2. Dumonteil E, Bottazzi ME, Zhan B, Heffernan MJ, Jones K, Valenzuela JG, Kamhawi S, Ortega J, Rosales SP, Lee BY, Bacon KM, Fleischer B, Slingsby BT, Cravioto MB, Tapia-Conyer R, Hotez PJ. 2012. Accelerating the development of a therapeutic vaccine for human Chagas disease: rationale and prospects. Expert Rev Vaccines 11:1043–1055. https://doi.org/10.1586/erv.12.85.
3. Hotez PJ, Bottazzi ME, Franco-Paredes C, Ault SK, Periago MR. 2008. The neglected tropical diseases of Latin America and the Caribbean: a review of disease burden and distribution and a roadmap for control and elimination. PLoS Negl Trop Dis 2:e300. https://doi.org/10.1371/journal.pntd.0000300.
4. Lee BY, Bacon KM, Bottazzi ME, Hotez PJ. 2013. Global economic burden of Chagas disease: a computational simulation model. Lancet Infect Dis 13:342–348. https://doi.org/10.1016/S1473-3099(13)70002-1.
5. Rassi A, Jr, Rassi A, Marin-Neto JA. 2010. Chagas disease. Lancet 375:1388–1402. https://doi.org/10.1016/S0140-6736(10)60061-X.
6. Bern C, Montgomery SP, Herwaldt BL, Rassi A, Jr, Marin-Neto JA, Dantas RO, Maguire JH, Acquatella H, Morillo C, Kirchhoff LV, Gilman RH, Reyes PA, Salvatella R, Moore AC. 2007. Evaluation and treatment of Chagas disease in the United States: a systematic review. JAMA 298:2171–2181. https://doi.org/10.1001/jama.298.18.2171.
7. Higuchi MDL, Benvenuti LA, Martins Reis M, Metzger M. 2003. Pathophysiology of the heart in Chagas' disease: current status and new developments. Cardiovasc Res 60:96–107. https://doi.org/10.1016/S0008-6363(03)00361-4.
8. Tanowitz HB, Machado FS, Jelicks LA, Shirani J, de Carvalho AC, Spray DC, Factor SM, Kirchhoff LV, Weiss LM. 2009. Perspectives on Trypanosoma cruzi-induced heart disease (Chagas disease). Prog Cardiovasc Dis 51:524–539. https://doi.org/10.1016/j.pcad.2009.02.001.
9. Biolo A, Ribeiro AL, Clausell N. 2010. Chagas cardiomyopathy—where do we stand after a hundred years? Prog Cardiovasc Dis 52:300–316. https://doi.org/10.1016/j.pcad.2009.11.008.
10. Acquatella H. 2007. Echocardiography in Chagas heart disease. Circulation 115:1124–1131. https://doi.org/10.1161/CIRCULATIONAHA.106.627323.
11. Le Loup G, Pialoux G, Lescure FX. 2011. Update in treatment of Chagas disease. Curr Opin Infect Dis 24:428–434. https://doi.org/10.1097/QCO.0b013e32834a667f.
12. Molina I, Gomez i Prat J, Salvador F, Trevino B, Sulleiro E, Serre N, Pou D, Roure S, Cabezos J, Valerio L, Blanco-Grau A, Sanchez-Montalva A, Vidal X, Pahissa A. 2014. Randomized trial of posaconazole and benznidazole for chronic Chagas' disease. N Engl J Med 370:1899–1908. https://doi.org/10.1056/NEJMoa1313122.
13. Viotti R, Vigliano C, Lococo B, Alvarez MG, Petti M, Bertocchi G, Armenti A. 2009. Side effects of benznidazole as treatment in chronic Chagas disease: fears and realities. Expert Rev Anti Infect Ther 7:157–163. https://doi.org/10.1586/14787210.7.2.157.
14. Pinazo MJ, Munoz J, Posada E, Lopez-Chejade P, Gallego M, Ayala E, del Cacho E, Soy D, Gascon J. 2010. Tolerance of benznidazole in treatment of Chagas' disease in adults. Antimicrob Agents Chemother 54:4896–4899. https://doi.org/10.1128/AAC.00537-10.
15. Issa VS, Bocchi EA. 2010. Antitrypanosomal agents: treatment or threat? Lancet 376:768. https://doi.org/10.1016/S0140-6736(10)61372-4. (Reply. 376:768–769. https://doi.org/10.1016/S0140-6736(10)61373-6.)

16. Molina J, Martins-Filho O, Brener Z, Romanha AJ, Loebenberg D, Urbina JA. 2000. Activities of the triazole derivative SCH 56592 (posaconazole) against drug-resistant strains of the protozoan parasite Trypanosoma (Schizotrypanum) cruzi in immunocompetent and immunosuppressed murine hosts. Antimicrob Agents Chemother 44:150–155. https://doi.org/10.1128/AAC.44.1.150-155.2000.
17. Morillo CA, Marin-Neto JA, Avezum A, Sosa-Estani S, Rassi A, Jr, Rosas F, Villena E, Quiroz R, Bonilla R, Britto C, Guhl F, Velazquez E, Bonilla L, Meeks B, Rao-Melacini P, Pogue J, Mattos A, Lazdins J, Rassi A, Connolly SJ, Yusuf S, BENEFIT Investigators. 2015. Randomized trial of benznidazole for chronic Chagas' cardiomyopathy. N Engl J Med 373:1295–1306. https://doi.org/10.1056/NEJMoa1507574.
18. Limon-Flores AY, Cervera-Cetina R, Tzec-Arjona JL, Ek-Macias L, Sanchez-Burgos G, Ramirez-Sierra MJ, Cruz-Chan JV, VanWynsberghe NR, Dumonteil E. 2010. Effect of a combination DNA vaccine for the prevention and therapy of Trypanosoma cruzi infection in mice: role of $CD4^+$ and $CD8^+$ T cells. Vaccine 28:7414–7419. https://doi.org/10.1016/j.vaccine.2010.08.104.
19. Quijano-Hernandez I, Dumonteil E. 2011. Advances and challenges towards a vaccine against Chagas disease. Hum Vaccin 7:1184–1191. https://doi.org/10.4161/hv.7.11.17016.
20. Dumonteil E, Escobedo-Ortegon J, Reyes-Rodriguez N, Arjona-Torres A, Ramirez-Sierra MJ. 2004. Immunotherapy of Trypanosoma cruzi infection with DNA vaccines in mice. Infect Immun 72:46–53. https://doi.org/10.1128/IAI.72.1.46-53.2004.
21. Sanchez-Burgos G, Mezquita-Vega RG, Escobedo-Ortegon J, Ramirez-Sierra MJ, Arjona-Torres A, Ouaissi A, Rodrigues MM, Dumonteil E. 2007. Comparative evaluation of therapeutic DNA vaccines against Trypanosoma cruzi in mice. FEMS Immunol Med Microbiol 50:333–341. https://doi.org/10.1111/j.1574-695X.2007.00251.x.
22. Gupta S, Garg NJ. 2013. TcVac3 induced control of Trypanosoma cruzi infection and chronic myocarditis in mice. PLoS One 8:e59434. https://doi.org/10.1371/journal.pone.0059434.
23. Pereira IR, Vilar-Pereira G, Marques V, da Silva AA, Caetano B, Moreira OC, Machado AV, Bruna-Romero O, Rodrigues MM, Gazzinelli RT, Lannes-Vieira J. 2015. A human type 5 adenovirus-based Trypanosoma cruzi therapeutic vaccine re-programs immune response and reverses chronic cardiomyopathy. PLoS Pathog 11:e1004594. https://doi.org/10.1371/journal.ppat.1004594.
24. Quijano-Hernandez IA, Castro-Barcena A, Vazquez-Chagoyan JC, Bolio-Gonzalez ME, Ortega-Lopez J, Dumonteil E. 2013. Preventive and therapeutic DNA vaccination partially protect dogs against an infectious challenge with Trypanosoma cruzi. Vaccine 31:2246–2252. https://doi.org/10.1016/j.vaccine.2013.03.005.
25. Martinez-Campos V, Martinez-Vega P, Ramirez-Sierra MJ, Rosado-Vallado M, Seid CA, Hudspeth EM, Wei J, Liu Z, Kwityn C, Hammond M, Ortega-Lopez J, Zhan B, Hotez PJ, Bottazzi ME, Dumonteil E. 2015. Expression, purification, immunogenicity, and protective efficacy of a recombinant Tc24 antigen as a vaccine against Trypanosoma cruzi infection in mice. Vaccine 33:4505–4512. https://doi.org/10.1016/j.vaccine.2015.07.017.
26. Barry MA, Wang Q, Jones KM, Heffernan MJ, Buhaya MH, Beaumier CM, Keegan BP, Zhan B, Dumonteil E, Bottazzi ME, Hotez PJ. 2016. A therapeutic nanoparticle vaccine against Trypanosoma cruzi in a BALB/c mouse model of Chagas disease. Hum Vaccin Immunother 12:976–987. https://doi.org/10.1080/21645515.2015.1119346.
27. Lee BY, Bacon KM, Wateska AR, Bottazzi ME, Dumonteil E, Hotez PJ. 2012. Modeling the economic value of a Chagas' disease therapeutic vaccine. Hum Vaccin Immunother 8:1293–1301. https://doi.org/10.4161/hv.20966.
28. Banchereau J, Steinman RM. 1998. Dendritic cells and the control of immunity. Nature 392:245–252. https://doi.org/10.1038/32588.
29. Medzhitov R. 2007. Recognition of microorganisms and activation of the immune response. Nature 449:819–826. https://doi.org/10.1038/nature06246.
30. Flores-Romo L. 2001. In vivo maturation and migration of dendritic cells. Immunology 102:255–262. https://doi.org/10.1046/j.1365-2567.2001.01204.x.
31. Joffre O, Nolte MA, Sporri R, Reis e Sousa C. 2009. Inflammatory signals in dendritic cell activation and the induction of adaptive immunity. Immunol Rev 227:234–247. https://doi.org/10.1111/j.1600-065X.2008.00718.x.
32. Belkaid Y, Oldenhove G. 2008. Tuning microenvironments: induction of regulatory T cells by dendritic cells. Immunity 29:362–371. https://doi.org/10.1016/j.immuni.2008.08.005.
33. Wu J, Horuzsko A. 2009. Expression and function of immunoglobulin-like transcripts on tolerogenic dendritic cells. Hum Immunol 70:353–356. https://doi.org/10.1016/j.humimm.2009.01.024.
34. Zhang J, Somani AK, Siminovitch KA. 2000. Roles of the SHP-1 tyrosine phosphatase in the negative regulation of cell signalling. Semin Immunol 12:361–378. https://doi.org/10.1006/smim.2000.0223.
35. Ramachandran IR, Song W, Lapteva N, Seethammagari M, Slawin KM, Spencer DM, Levitt JM. 2011. The phosphatase SRC homology region 2 domain-containing phosphatase-1 is an intrinsic central regulator of dendritic cell function. J Immunol 186:3934–3945. https://doi.org/10.4049/jimmunol.1001675.
36. Beaumier CM, Gillespie PM, Strych U, Hayward T, Hotez PJ, Bottazzi ME. 2016. Status of vaccine research and development of vaccines for Chagas disease. Vaccine 34:2996–3000. https://doi.org/10.1016/j.vaccine.2016.03.074.
37. Ono T, Yamaguchi Y, Oguma T, Takayama E, Takashima Y, Tadakuma T, Miyahira Y. 2012. Actively induced antigen-specific $CD8^+$ T cells by epitope-bearing parasite pre-infection but not prime/boost virus vector vaccination could ameliorate the course of Plasmodium yoelii blood-stage infection. Vaccine 30:6270–6278. https://doi.org/10.1016/j.vaccine.2012.08.009.
38. Casimiro DR, Chen L, Fu TM, Evans RK, Caulfield MJ, Davies ME, Tang A, Chen M, Huang L, Harris V, Freed DC, Wilson KA, Dubey S, Zhu DM, Nawrocki D, Mach H, Troutman R, Isopi L, Williams D, Hurni W, Xu Z, Smith JG, Wang S, Liu X, Guan L, Long R, Trigona W, Heidecker GJ, Perry HC, Persaud N, Toner TJ, Su Q, Liang X, Youil R, Chastain M, Bett AJ, Volkin DB, Emini EA, Shiver JW. 2003. Comparative immunogenicity in rhesus monkeys of DNA plasmid, recombinant vaccinia virus, and replication-defective adenovirus vectors expressing a human immunodeficiency virus type 1 gag gene. J Virol 77:6305–6313. https://doi.org/10.1128/JVI.77.11.6305-6313.2003.
39. Park D, Lapteva N, Seethammagari M, Slawin KM, Spencer DM. 2006. An essential role for Akt1 in dendritic cell function and tumor immunotherapy. Nat Biotechnol 24:1581–1590. https://doi.org/10.1038/nbt1262.
40. Narayanan P, Lapteva N, Seethammagari M, Levitt JM, Slawin KM, Spencer DM. 2011. A composite MyD88/CD40 switch synergistically activates mouse and human dendritic cells for enhanced antitumor efficacy. J Clin Invest 121:1524–1534. https://doi.org/10.1172/JCI44327.
41. Konduri V, Li D, Halpert MM, Liang D, Liang Z, Chen Y, Fisher WE, Paust S, Levitt JM, Yao QC, Decker WK. 2016. Chemo-immunotherapy mediates durable cure of orthotopic KrasG12D/p53−/− pancreatic ductal adenocarcinoma. Oncoimmunology 5:e1213933. https://doi.org/10.1080/2162402X.2016.1213933.
42. Decker WK, Xing D, Li S, Robinson SN, Yang H, Yao X, Segall H, McMannis JD, Komanduri KV, Champlin RE, Shpall EJ. 2006. Double loading of dendritic cell MHC class I and MHC class II with an AML antigen repertoire enhances correlates of T-cell immunity in vitro via amplification of T-cell help. Vaccine 24:3203–3216. https://doi.org/10.1016/j.vaccine.2006.01.029.
43. Decker WK, Xing D, Li S, Robinson SN, Yang H, Steiner D, Komanduri KV, Shpall EJ. 2009. Th-1 polarization is regulated by dendritic-cell comparison of MHC class I and class II antigens. Blood 113:4213–4223. https://doi.org/10.1182/blood-2008-10-185470.
44. Hanks BA, Jiang J, Singh RA, Song W, Barry M, Huls MH, Slawin KM, Spencer DM. 2005. Re-engineered CD40 receptor enables potent pharmacological activation of dendritic-cell cancer vaccines in vivo. Nat Med 11:130–137. https://doi.org/10.1038/nm1183.
45. Nesterovitch AB, Szanto S, Gonda A, Bardos T, Kis-Toth K, Adarichev VA, Olasz K, Ghassemi-Najad S, Hoffman MD, Tharp MD, Mikecz K, Glant TT. 2011. Spontaneous insertion of a b2 element in the ptpn6 gene drives a systemic autoinflammatory disease in mice resembling neutrophilic dermatosis in humans. Am J Pathol 178:1701–1714. https://doi.org/10.1016/j.ajpath.2010.12.053.
46. Aoki K, Didomenico E, Sims NA, Mukhopadhyay K, Neff L, Houghton A, Amling M, Levy JB, Horne WC, Baron R. 1999. The tyrosine phosphatase SHP-1 is a negative regulator of osteoclastogenesis and osteoclast resorbing activity: increased resorption and osteopenia in me(v)/me(v) mutant mice. Bone 25:261–267. https://doi.org/10.1016/S8756-3282(99)00174-X.
47. Kim JH, Lee SR, Li LH, Park HJ, Park JH, Lee KY, Kim MK, Shin BA, Choi SY. 2011. High cleavage efficiency of a 2A peptide derived from porcine teschovirus-1 in human cell lines, zebrafish and mice. PLoS One 6:e18556. https://doi.org/10.1371/journal.pone.0018556.
48. Cencig S, Coltel N, Truyens C, Carlier Y. 2011. Parasitic loads in tissues of

mice infected with Trypanosoma cruzi and treated with AmBisome. PLoS Negl Trop Dis 5:e1216. https://doi.org/10.1371/journal.pntd.0001216.
49. Quijano-Hernandez IA, Bolio-Gonzalez ME, Rodriguez-Buenfil JC, Ramirez-Sierra MJ, Dumonteil E. 2008. Therapeutic DNA vaccine against Trypanosoma cruzi infection in dogs. Ann N Y Acad Sci 1149:343–346. https://doi.org/10.1196/annals.1428.098.
50. Garzoni LR, Adesse D, Soares MJ, Rossi MID, Borojevic R, de Meirelles MDNL. 2008. Fibrosis and hypertrophy induced by Trypanosoma cruzi in a three-dimensional cardiomyocyte-culture system. J Infect Dis 197: 906–915. https://doi.org/10.1086/528373.
51. Udoko AN, Johnson CA, Dykan A, Rachakonda G, Villalta F, Mandape SN, Lima MF, Pratap S, Nde PN. 2016. Early regulation of profibrotic genes in primary human cardiac myocytes by Trypanosoma cruzi. PLoS Negl Trop Dis 10:e0003747. https://doi.org/10.1371/journal.pntd.0003747.
52. Waghabi MC, Keramidas M, Feige JJ, Araujo-Jorge TC, Bailly S. 2005. Activation of transforming growth factor beta by Trypanosoma cruzi. Cell Microbiol 7:511–517. https://doi.org/10.1111/j.1462-5822.2004.00481.x.
53. Lin J, Patel SR, Cheng X, Cho EA, Levitan I, Ullenbruch M, Phan SH, Park JM, Dressler GR. 2005. Kielin/chordin-like protein, a novel enhancer of BMP signaling, attenuates renal fibrotic disease. Nat Med 11:387–393. https://doi.org/10.1038/nm1217.
54. Shi Y, Massague J. 2003. Mechanisms of TGF-beta signaling from cell membrane to the nucleus. Cell 113:685–700. https://doi.org/10.1016/S0092-8674(03)00432-X.
55. Neilson EG. 2005. Setting a trap for tissue fibrosis. Nat Med 11:373–374. https://doi.org/10.1038/nm0405-373.
56. Aparicio-Burgos JE, Ochoa-Garcia L, Zepeda-Escobar JA, Gupta S, Dhiman M, Martinez JS, de Oca-Jimenez RM, Val Arreola M, Barbabosa-Pliego A, Vazquez-Chagoyan JC, Garg NJ. 2011. Testing the efficacy of a multi-component DNA-prime/DNA-boost vaccine against Trypanosoma cruzi infection in dogs. PLoS Negl Trop Dis 5:e1050. https://doi.org/10.1371/journal.pntd.0001050.
57. Carvalho CM, Andrade MC, Xavier SS, Mangia RH, Britto CC, Jansen AM, Fernandes O, Lannes-Vieira J, Bonecini-Almeida MG. 2003. Chronic Chagas' disease in rhesus monkeys (Macaca mulatta): evaluation of parasitemia, serology, electrocardiography, echocardiography, and radiology. Am J Trop Med Hyg 68:683–691.
58. Pisharath H, Zao CL, Kreeger J, Portugal S, Kawabe T, Burton T, Tomaeck L, Shoieb A, Campbell BM, Franco J. 2013. Immunopathologic characterization of naturally acquired Trypanosoma cruzi infection and cardiac sequalae [*sic*] in cynomolgus macaques (Macaca fascicularis). J Am Assoc Lab Anim Sci 52:545–552.
59. Bryan MA, Guyach SE, Norris KA. 2010. Specific humoral immunity versus polyclonal B cell activation in Trypanosoma cruzi infection of susceptible and resistant mice. PLoS Negl Trop Dis 4:e733. https://doi.org/10.1371/journal.pntd.0000733.
60. el Bouhdidi A, Truyens C, Rivera MT, Bazin H, Carlier Y. 1994. Trypanosoma cruzi infection in mice induces a polyisotypic hypergammaglobulinaemia and parasite-specific response involving high IgG2a concentrations and highly avid IgG1 antibodies. Parasite Immunol 16:69–76. https://doi.org/10.1111/j.1365-3024.1994.tb00325.x.
61. Padilla AM, Bustamante JM, Tarleton RL. 2009. $CD8^+$ T cells in Trypanosoma cruzi infection. Curr Opin Immunol 21:385–390. https://doi.org/10.1016/j.coi.2009.07.006.
62. Martin D, Tarleton R. 2004. Generation, specificity, and function of $CD8^+$ T cells in Trypanosoma cruzi infection. Immunol Rev 201:304–317. https://doi.org/10.1111/j.0105-2896.2004.00183.x.
63. Farrow AL, Rachakonda G, Gu L, Krendelchtchikova V, Nde PN, Pratap S, Lima MF, Villalta F, Matthews QL. 2014. Immunization with hexon modified adenoviral vectors integrated with gp83 epitope provides protection against Trypanosoma cruzi infection. PLoS Negl Trop Dis 8:e3089. https://doi.org/10.1371/journal.pntd.0003089.
64. Avraham T, Zampell JC, Yan A, Elhadad S, Weitman ES, Rockson SG, Bromberg J, Mehrara BJ. 2013. Th2 differentiation is necessary for soft tissue fibrosis and lymphatic dysfunction resulting from lymphedema. FASEB J 27:1114–1126. https://doi.org/10.1096/fj.12-222695.
65. Coutinho HM, Acosta LP, Wu HW, McGarvey ST, Su L, Langdon GC, Jiz MA, Jarilla B, Olveda RM, Friedman JF, Kurtis JD. 2007. Th2 cytokines are associated with persistent hepatic fibrosis in human Schistosoma japonicum infection. J Infect Dis 195:288–295. https://doi.org/10.1086/510313.
66. Pesce JT, Ramalingam TR, Mentink-Kane MM, Wilson MS, El Kasmi KC, Smith AM, Thompson RW, Cheever AW, Murray PJ, Wynn TA. 2009. Arginase-1-expressing macrophages suppress Th2 cytokine-driven inflammation and fibrosis. PLoS Pathog 5:e1000371. https://doi.org/10.1371/journal.ppat.1000371.
67. Barron L, Wynn TA. 2011. Fibrosis is regulated by Th2 and Th17 responses and by dynamic interactions between fibroblasts and macrophages. Am J Physiol Gastrointest Liver Physiol 300:G723–G728. https://doi.org/10.1152/ajpgi.00414.2010.
68. Lei L, Zhao C, Qin F, He ZY, Wang X, Zhong XN. 2016. Th17 cells and IL-17 promote the skin and lung inflammation and fibrosis process in a bleomycin-induced murine model of systemic sclerosis. Clin Exp Rheumatol 34(Suppl 100):S14–S22.
69. Ray S, De Salvo C, Pizarro TT. 2014. Central role of IL-17/Th17 immune responses and the gut microbiota in the pathogenesis of intestinal fibrosis. Curr Opin Gastroenterol 30:531–538. https://doi.org/10.1097/MOG.0000000000000119.
70. Wang B, Liang S, Wang Y, Zhu XQ, Gong W, Zhang HQ, Li Y, Xia CM. 2015. Th17 down-regulation is involved in reduced progression of schistosomiasis fibrosis in ICOSL KO mice. PLoS Negl Trop Dis 9:e0003434. https://doi.org/10.1371/journal.pntd.0003434.
71. Gowdy KM, Nugent JL, Martinu T, Potts E, Snyder LD, Foster WM, Palmer SM. 2012. Protective role of T-bet and Th1 cytokines in pulmonary graft-versus-host disease and peribronchiolar fibrosis. Am J Respir Cell Mol Biol 46:249–256. https://doi.org/10.1165/rcmb.2011-0131OC.
72. Tao FF, Yang YF, Wang H, Sun XJ, Luo J, Zhu X, Liu F, Wang Y, Su C, Wu HW, Zhang ZS. 2009. Th1-type epitopes-based cocktail PDDV attenuates hepatic fibrosis in C57BL/6 mice with chronic Schistosoma japonicum infection. Vaccine 27:4110–4117. https://doi.org/10.1016/j.vaccine.2009.04.073.
73. Zhang LH, Pan JP, Yao HP, Sun WJ, Xia DJ, Wang QQ, He L, Wang J, Cao X. 2001. Intrasplenic transplantation of IL-18 gene-modified hepatocytes: an effective approach to reverse hepatic fibrosis in schistosomiasis through induction of dominant Th1 response. Gene Ther 8:1333–1342. https://doi.org/10.1038/sj.gt.3301524.
74. Bustamante JM, Craft JM, Crowe BD, Ketchie SA, Tarleton RL. 2014. New, combined, and reduced dosing treatment protocols cure Trypanosoma cruzi infection in mice. J Infect Dis 209:150–162. https://doi.org/10.1093/infdis/jit420.
75. Cencig S, Coltel N, Truyens C, Carlier Y. 2012. Evaluation of benznidazole treatment combined with nifurtimox, posaconazole or AmBisome in mice infected with Trypanosoma cruzi strains. Int J Antimicrob Agents 40:527–532. https://doi.org/10.1016/j.ijantimicag.2012.08.002.
76. Kemnade JO, Seethammagari M, Narayanan P, Levitt JM, McCormick AA, Spencer DM. 2012. Off-the-shelf adenoviral-mediated immunotherapy via bicistronic expression of tumor antigen and iMyD88/CD40 adjuvant. Mol Ther 20:1462–1471. https://doi.org/10.1038/mt.2012.48.
77. Konduri V, Decker WK, Halpert MM, Gilbert B, Safdar A. 2013. Modeling dendritic cell vaccination for influenza prophylaxis: potential applications for niche populations. J Infect Dis 207:1764–1772. https://doi.org/10.1093/infdis/jit087.
78. Melo MF, Moreira OC, Tenorio P, Lorena V, Lorena-Rezende I, Oliveira W, Jr, Gomes Y, Britto C. 2015. Usefulness of real time PCR to quantify parasite load in serum samples from chronic Chagas disease patients. Parasit Vectors 8:154. https://doi.org/10.1186/s13071-015-0770-0.
79. Piron M, Fisa R, Casamitjana N, Lopez-Chejade P, Puig L, Verges M, Gascon J, Gomez i Prat J, Portus M, Sauleda S. 2007. Development of a real-time PCR assay for Trypanosoma cruzi detection in blood samples. Acta Trop 103:195–200. https://doi.org/10.1016/j.actatropica.2007.05.019.
80. Gangisetty O, Reddy DS. 2009. The optimization of TaqMan real-time RT-PCR assay for transcriptional profiling of GABA-A receptor subunit plasticity. J Neurosci Methods 181:58–66. https://doi.org/10.1016/j.jneumeth.2009.04.016.
81. Caldas S, Caldas IS, Diniz LDF, de Lima WG, Oliveira RDP, Cecilio AB, Ribeiro I, Talvani A, Bahia MT. 2012. Real-time PCR strategy for parasite quantification in blood and tissue samples of experimental Trypanosoma cruzi infection. Acta Trop 123:170–177. https://doi.org/10.1016/j.actatropica.2012.05.002.